
MAGNETISM
AND FERROELECTRICITY

Ground State and Properties of Ferroelectric Superlattices Based on Crystals of the Perovskite Family

A. I. Lebedev

Moscow State University, Moscow, 119991 Russia

e-mail: swan@scon155.phys.msu.ru

Received November 25, 2009

Abstract—The crystal structure of the ground state of ten free-standing ferroelectric superlattices based on crystals with the perovskite structure ($\text{BaTiO}_3/\text{SrTiO}_3$, $\text{PbTiO}_3/\text{SrTiO}_3$, $\text{PbTiO}_3/\text{PbZrO}_3$, $\text{SrZrO}_3/\text{SrTiO}_3$, $\text{PbZrO}_3/\text{BaZrO}_3$, $\text{BaTiO}_3/\text{BaZrO}_3$, $\text{PbTiO}_3/\text{BaTiO}_3$, $\text{BaTiO}_3/\text{CaTiO}_3$, $\text{KNbO}_3/\text{KTaO}_3$, and $\text{KNbO}_3/\text{NaNbO}_3$) was calculated from first principles within the density functional theory taking into account criteria for stability of the structures with respect to acoustic and optical distortions. It was shown that the ground state in all the considered superlattices corresponds to the ferroelectric phase. It was found that the polarization vector has a tendency toward a tilt to the plane of the superlattice layers, which makes it possible to decrease the electrostatic and elastic energy in the superlattices consisting of materials with different ferroelectric properties. The importance of the inclusion of structural distortions due to unstable phonons at the Brillouin zone boundary, which, in a number of cases, lead to significant changes in ferroelectric and dielectric properties of the superlattices, was demonstrated.

DOI: 10.1134/S1063783410070218

1. INTRODUCTION

Ferroelectric superlattices, which have been studied for a significantly shorter period of time than semiconductor and magnetic superlattices, have attracted much attention. It has appeared that, for these artificial structures, many physical parameters, such as the Curie temperature, spontaneous polarization, dielectric constant, and nonlinear dielectric and optical susceptibilities, exceed considerably those of bulk crystals and thin films of solid solutions of the corresponding composition. The search for new approaches that will enable one to improve noticeably the characteristics of ferroelectrics is of great scientific and applied importance. Since many properties of ferroelectric superlattices are still poorly studied experimentally, theoretical calculations occupy a significant place in the modern investigations of these structures.

The reliable prediction of the physical properties of superlattices from first principles and the correct interpretation of the experimental results require knowledge of the ground state of the superlattices. A number of calculations of the ground state of the ferroelectric superlattices based on crystals with the perovskite structure are available in the literature; however, in the majority of cases, the calculations have been restricted to the determination of a phase (among several ferroelectric phases with a specified symmetry) in which the relaxation of atomic positions and the unit cell parameters results in a structure with the lowest total energy. Unfortunately, this approach cannot be considered as quite correct, because the found solu-

tions can correspond not to the true energy minimum (the ground state) but to the saddle point only. An example of such calculations can be provided by calculations of the properties of the $\text{KNbO}_3/\text{KTaO}_3$, $\text{PbTiO}_3/\text{BaTiO}_3$, $\text{PbTiO}_3/\text{SrTiO}_3$, $\text{PbTiO}_3/\text{PbZrO}_3$, $\text{SrZrO}_3/\text{SrTiO}_3$, $\text{BaTiO}_3/\text{CaTiO}_3$, and $\text{KNbO}_3/\text{NaNbO}_3$ superlattices, which will be discussed below.

It is well known that, in addition to the ferroelectric instability, perovskite crystals often exhibit a structural instability associated with the presence of phonons at the Brillouin zone boundary. Therefore, the inclusion of the competition between the ferroelectric and structural instabilities is of fundamental importance for the correct prediction of the crystal properties. A substantial influence of this competition on the crystal properties can be demonstrated using CaTiO_3 as an example. In the parent cubic phase $Pm\bar{3}m$, calcium titanate exhibits a ferroelectric instability (the frequency of the Γ_{15} mode is equal to $165i \text{ cm}^{-1}$ [1]); however, a stronger structural instability with respect to phonons at the R and M points of the Brillouin zone results in a reduction of the symmetry of the structure to orthorhombic and in a complete suppression of the ferroelectric instability (the frequency of the two softest modes with symmetry B_{1u} and B_{3u} in orthorhombic CaTiO_3 is equal to 82 cm^{-1} [2]).

In the present work, we investigated properties of ten short-period ferroelectric superlattices based on crystals of the perovskite family, for which experimental data or results of theoretical calculations are avail-

Table 1. Electronic configurations of atoms and parameters used for constructing pseudopotentials: r_s , r_p , r_d , and r_f are the radii of the pseudopotential core for the s , p , d , and f projections, respectively; q_s , q_p , q_d , and q_f are the boundary wave vectors used for optimizing the pseudopotential; and r_{\min} , r_{\max} , and V_{loc} are the range and depth of the correcting local potential (parameters are given in Hartree atomic units, and the energy is given in Ry)

| Atom | Configuration | r_s | r_p | r_d | r_f | q_s | q_p | q_d | q_f | r_{\min} | r_{\max} | V_{loc} |
|------|----------------------------|-------|-------|-------|-------|-------|-------|-------|-------|------------|------------|------------------|
| Na | $2s^2 2p^6 3s^0 3p^0$ | 1.18 | 1.60 | — | — | 7.07 | 7.87 | — | — | 0.01 | 1.08 | 1.2 |
| K | $3s^2 3p^6 3d^0 4s^0 4p^0$ | 1.38 | 1.42 | 1.44 | — | 7.47 | 7.27 | 7.07 | — | 0.01 | 1.40 | 0.65 |
| Zr | $4s^2 4p^6 4d^0 5s^0$ | 1.58 | 1.74 | 1.78 | — | 7.27 | 7.07 | 7.07 | — | 0.01 | 1.30 | 4.04 |
| Nb | $4s^2 4p^6 4d^0 5s^0$ | 1.76 | 1.76 | 1.76 | — | 7.07 | 7.07 | 7.07 | — | 0.01 | 1.48 | 2.05 |
| Ta | $4f^4 4s^2 5p^6 5d^0 6s^0$ | 1.74 | 1.74 | 1.74 | 1.58 | 7.07 | 7.07 | 7.07 | 8.5 | — | — | — |

able in the literature: BaTiO₃/SrTiO₃ (see references in [3] and also [4–16]), PbTiO₃/SrTiO₃ [17–22], PbTiO₃/PbZrO₃ [23–30], SrZrO₃/SrTiO₃ [15, 31–34], PbZrO₃/BaZrO₃ [35, 36], BaTiO₃/BaZrO₃ [15, 37, 38], PbTiO₃/BaTiO₃ [39–42], BaTiO₃/CaTiO₃ [43, 44], KNbO₃/KTaO₃ [45–53], and KNbO₃/NaNbO₃ [54]. By sequentially performing the relaxation procedure for positions of atoms and the unit cell parameters with the subsequent analysis of the stability of the obtained structures for each of the aforementioned superlattices, we determined the ground state, calculated main ferroelectric and dielectric properties, and compared the results of the calculations with the data available in the literature.

The purpose of this work was to understand whether the structural data known for many solid solutions can be used for predicting the structure of the ground state of the corresponding superlattices and to reveal how strongly the structural instability manifesting itself in the superlattices will affect their ferroelectric properties. The data obtained can be used as a guide in interpreting the results of future experimental studies of superlattices.

2. CALCULATION TECHNIQUE

The calculations were carried out from first principles within the density functional theory with the pseudopotentials and the plane-wave expansion of wave functions as implemented in the ABINIT code [55]. The exchange–correlation interaction was described within the local-density approximation according to the procedure proposed in [56]. As pseudopotentials, we used the optimized separable nonlocal pseudopotentials [57] generated with the OPIUM code [58] to which the local potential was added in order to improve their transferability [59]. The pseudopotentials for Sr, Ba, Ca, Pb, Ti, and O atoms were taken from [1]; the parameters used in constructing the pseudopotentials for new atoms are presented in Table 1. Among these atoms, the special place is occupied by tantalum, for which the pseudopotential initially constructed without taking into account the $4f$ shell led to appreciably underestimated

values of the lattice parameter for KTaO₃ and metallic tantalum. Consequently, the completely filled $4f$ shell of the tantalum atom was taken into account in the pseudopotential used in our calculations. The maximum energy of plane waves was equal to 40 Ha for the KNbO₃/KTaO₃ superlattice and 30 Ha for other superlattices.¹ The integration over the Brillouin zone was performed using the $8 \times 8 \times 4$ k -point mesh generated for ten-atom unit cells and using the $6 \times 6 \times 4$ k -point mesh generated for twenty-atom unit cells according to the Monkhorst–Pack scheme [60]. The relaxation of atomic positions was performed until the Hellmann–Feynman forces decreased below 5×10^{-6} Ha/Bohr. The phonon spectra and the dielectric and elastic properties were calculated in the framework of the density functional theory according to the formulas obtained from the perturbation theory. The phonon contribution to the static dielectric constant tensor was calculated from the determined frequencies of phonons and effective atomic charges.

The spontaneous polarization P_s was calculated by the Berry phase method. Since the unit cell volume Ω in the considered superlattices was 2–4 times larger than that in the parent crystals with the perovskite structure and the value of the polarization in the Berry phase calculations was determined with an accuracy of the “polarization quantum” $e\mathbf{R}/\Omega$ (where \mathbf{R} is the lattice vector [61]), the polarization was calculated for both the equilibrium polar structure and the structures in which the polar displacements of atoms (with respect to their positions in the paraelectric phase) were equal to one-half and one-fourth of the maximum polar displacements. This enabled us to reconstruct the “trajectory of motion” of the Berry phase and to find the correct value of the polarization.

The search for the ground state of the superlattice was performed as follows. First, the equilibrium structure of the nonpolar phase with space group $P4/mmm$ was determined by minimizing the Hellmann–Feynman forces. Then, for this structure, the frequencies of the phonon spectrum were calculated at the Γ point.

¹ In this paper, some parameters used in the calculations are given in Hartree atomic units.

The ground state of the superlattice, which has the lowest total energy, is characterized by positive values of all frequencies of optical phonons at all points of the Brillouin zone and the structure itself should be mechanically stable. The search for the ground state was started with the determination of the structure for which frequencies of all optical phonons at the Γ point would be positive. Since in the phonon spectrum of the $P4/mmm$ phase of all the investigated superlattices, there were unstable modes at the Γ point (with imaginary mode frequencies), small perturbations corresponding to the eigenvector of the least stable of these modes were introduced into the structure and the equilibrium structure of the low-symmetry phase was determined by means of the relaxation of atomic positions and the unit cell parameters. In the case of the doubly degenerate mode E_u , we considered two types of distortions described by the order parameters $(\eta, 0)$ and (η, η) .² The analysis of the phonon spectrum and the search for a new low-symmetry structure were continued until the structure with positive frequencies of all optical phonons at the Γ point was found. For this structure, we calculated the elastic moduli tensor $C_{\mu\nu}$ and checked whether the structure is mechanically stable (the determinant of the 6-by-6 matrix of the elastic moduli in the Voigt notation and all leading principal minors should be positive). This structure will be referred to as the “ferroelectric ground state.”

For the “ferroelectric ground state,” the existence of other unstable modes in the structure under consideration was checked by calculating the phonon frequencies at high-symmetry points at the Brillouin zone boundary. If such an instability was revealed, then, in accordance with the position of the least stable mode among these unstable modes (usually, it was the $M(S)$ point³), a new unit cell with the double volume was constructed, small atomic displacements corresponding to the least stable of the modes under consideration were introduced into this unit cell, and the equilibrium structure was determined by means of the relaxation of atomic positions and the unit cell parameters. The analysis of the phonon spectrum and the search for new low-symmetry structures were continued until the structure with positive frequencies of all phonons at the center and high-symmetry points at the boundary of the Brillouin zone was found. For this structure, we calculated the elastic moduli tensor and checked whether the structure is mechanically stable.

² When the fourth-degree invariants in the expansion of the energy in powers of the atomic displacements are taken into account, the energy minimum is reached for one of the aforementioned order parameters.

³ For the points of the Brillouin zone of the low-symmetry phases, we will use the notations of the points of the tetragonal reciprocal lattice for base-centered orthorhombic and monoclinic lattices and its own notations for the simple orthorhombic lattice. The M point of the tetragonal lattice is equivalent to the S point of the orthorhombic lattice.

This structure corresponded to the structure of the true ground state.

Up to now, the described complete scheme of the search for the ground state of ferroelectric superlattices has been used only two times: for the $\text{PbTiO}_3/\text{SrTiO}_3$ superlattice in [21] and the $\text{BaTiO}_3/\text{SrTiO}_3$ superlattice in the author's previous work [3].

3. RESULTS OF THE CALCULATIONS

The search for the ground state in superlattices with taking into account all possible instabilities of the phonon spectrum and with the simultaneous inclusion of the influence of the substrate-induced strain is a very laborious task. In this paper, we will restrict our consideration to the search for the ground state for the shortest period superlattices which are grown in the $\langle 001 \rangle$ direction and consist of alternating layers of two components, each having the thickness equal to one unit cell. We will mainly consider properties of free-standing superlattices, i.e., superlattices free of substrate-induced strains; however, in a number of cases (for comparison with results of investigations of other authors), we will consider superlattices with other periods and substrate-supported superlattices.

The importance of research on the properties of free-standing superlattices is associated with the fact that the coherently strained state in superlattices is stable only in very thin layers; in films with the layer thickness larger than a certain critical thickness, there arise misfit dislocations and the strained state relaxes. The characteristic value of the critical thickness for the considered superlattices is equal to ~ 100 Å; therefore, we can suppose that the majority of the experimentally studied superlattices with the thickness lying in the range 320–4500 Å are in a relaxed state close to the state of the corresponding free-standing superlattice.

We consider first the results obtained from calculations of the structure of low-symmetry phases without regard for their distortions described by phonons at the Brillouin zone boundary. The phonon spectrum of one of the investigated free-standing superlattices, i.e., $\text{PbTiO}_3/\text{BaTiO}_3$, in the paraelectric phase ($P4/mmm$) and in the ground state (the $Pmm2$ phase) is shown in Fig. 1 (the dispersion curves were obtained by the extrapolation of the data calculated at 12 and 18 irreducible points of the Brillouin zone, respectively). It is seen that, in the phonon spectrum of the paraelectric phase, there are two unstable phonons at the Γ point. The frequencies and symmetry of the unstable phonons at the Γ point in the $P4/mmm$ phase for ten superlattices studied in this work are presented in Table 2. It follows from the table that the phonon spectra of all the investigated superlattices are characterized by unstable ferroelectric modes with symmetry A_{2u} (with the polarization of vibrations along the tetragonal axis) and E_u (with the polarization in the xy

plane) that arise from the unstable mode Γ_{15} , which is characteristic of many perovskites. With the exception of the $\text{BaTiO}_3/\text{BaZrO}_3$ superlattice in which only one mode, namely, E_u , is unstable, in the other superlattices, both modes are unstable simultaneously, so that the E_u mode is always less stable. Therefore, one can expect that the symmetry of the polar phase, most likely, will be lower than tetragonal. In phonon spectra of three superlattices, the appearance of three unstable modes with symmetry E_g and B_{2u} at the Γ point indicates other possible distortions of the structure; however, the instability of these modes is weaker and the phases distorted in a corresponding manner (with space groups $P2/m$, $P\bar{1}$, and $P\bar{4}m2$) have a higher energy as compared to the polar phase.

The symmetry of the “ferroelectric ground state” and the orientation of the polarization vector with respect to the axes of the tetragonal lattice of the paraelectric phase according to the results obtained from calculations for all superlattices are presented in Table 2. It can be seen that the “ferroelectric ground state” has symmetry $Amm2$, $Pmm2$, Cm , $P4mm$, and $P4mm$. We think that, in the $\text{PbZrO}_3/\text{BaZrO}_3$ superlattice, the symmetry of the “ferroelectric ground state” is $Pmm2$, even though the minimum of the total energy was reached by the rotation of the polarization vector through an angle of 0.02° in the xz plane with respect to the polar x axis of the $Pmm2$ phase (in the setting $P2mm$).

It should be noted that the criterion for mechanical stability is actually important for the verification as to whether the structure under investigation is the ground state. In particular, for the $\text{SrZrO}_3/\text{SrTiO}_3$ superlattice, the “ferroelectric ground state” is the $P4mm$ phase, which has the lowest energy and is characterized by positive frequencies of all optical phonons at the Γ point. It was surprising to reveal that the $Amm2$ phase of this superlattice, which has a higher energy, is

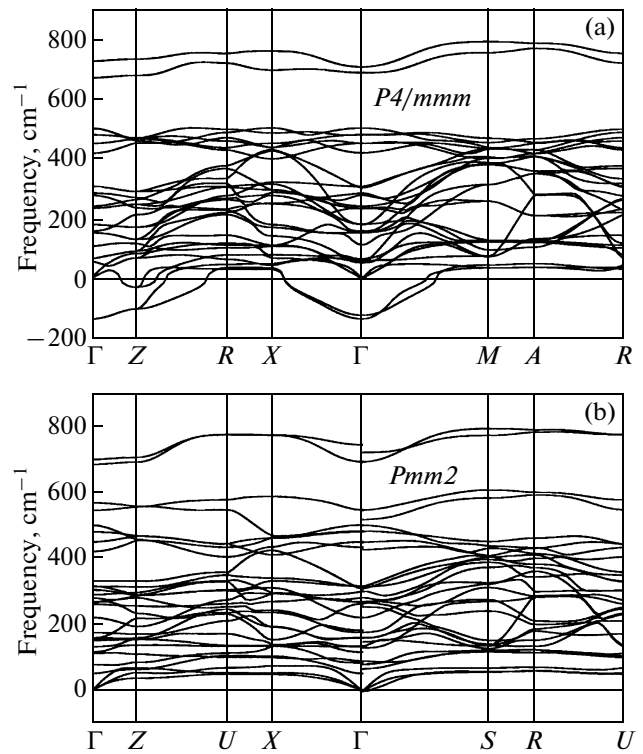


Fig. 1. Phonon spectrum of the free-standing superlattice $(\text{PbTiO}_3)_1(\text{BaTiO}_3)_1$ in (a) the paraelectric phase $P4/mmm$ and (b) the ground state, i.e., the ferroelectric phase $Pmm2$.

also characterized by positive frequencies of all phonons at the Γ point. The only indication of the instability of this phase lies in the fact that it is mechanically unstable: the quadratic form, which expresses the strain energy of the crystal in terms of the strain tensor components, was not positive definite ($C_{12} > C_{11} = C_{22}$). The criterion for mechanical stability turned out to be important for other systems: the

Table 2. Relative difference in the lattice parameters $\Delta a/\bar{a}$ for the starting components, enthalpy of mixing ΔH , unstable optical phonons at the Γ point in the paraelectric phase $P4/mmm$, space group, and orientation of the polarization vector in the “ferroelectric ground state” of the investigated superlattices

| Superlattice | $\Delta a/\bar{a}$, % | ΔH , meV | Unstable phonons at the Γ point, cm^{-1} | Space group |
|---------------------------------|------------------------|------------------|--|--------------|
| $\text{BaTiO}_3/\text{SrTiO}_3$ | 2.09 | +2.9 | $102i (E_u)$, $97i (A_{2u})$ | $Cm (xxz)$ |
| $\text{KNbO}_3/\text{KTaO}_3$ | 1.16 | +3.2 | $143i (E_u)$, $106i (A_{2u})$ | $Cm (xxz)$ |
| $\text{KNbO}_3/\text{NaNbO}_3$ | 0.91 | -1.5 | $191i (E_u)$, $189i (A_{2u})$, $125i (E_g)$ | $Amm2 (xx0)$ |
| $\text{PbTiO}_3/\text{SrTiO}_3$ | 0.76 | -3.3 | $119i (E_u)$, $107i (A_{2u})$ | $Pmm2 (x00)$ |
| $\text{PbTiO}_3/\text{PbZrO}_3$ | 5.12 | +78 | $201i (E_u)$, $181i (A_{2u})$, $153i (B_{2u})$, $97i (E_u)$, $33i (E_g)$ | $Cm (xxz)$ |
| $\text{SrZrO}_3/\text{SrTiO}_3$ | 5.54 | +110 | $190i (E_u)$, $162i (B_{2u})$, $148i (A_{2u})$, $100i (E_u)$ | $P4mm (00z)$ |
| $\text{PbZrO}_3/\text{BaZrO}_3$ | 0.98 | -1.9 | $111i (E_u)$, $79i (A_{2u})$ | $Pmm2 (x00)$ |
| $\text{BaTiO}_3/\text{BaZrO}_3$ | 4.76 | +72 | $248i (E_u)$ | $Amm2 (xx0)$ |
| $\text{PbTiO}_3/\text{BaTiO}_3$ | 1.33 | -0.4 | $135i (E_u)$, $123i (A_{2u})$ | $Pmm2 (x00)$ |
| $\text{BaTiO}_3/\text{CaTiO}_3$ | 3.35 | +6.8 | $145i (E_u)$, $106i (A_{2u})$ | $Pmm2 (x00)$ |

Table 3. Frequencies of all unstable phonons or the lowest frequency stable phonon at different points of the Brillouin zone for the “ferroelectric ground state” of the investigated ferroelectric superlattices (the space groups corresponding to the true ground state are printed in boldface)

| Superlattice | Space group | Phonon frequencies, cm^{-1} | | | | | | | |
|--|-------------|--------------------------------------|-----|------|-----|---------------|-----|-----|----------|
| | | Γ | Z | X | | M | R | | A |
| BaTiO ₃ /SrTiO ₃ | Cm | 54 | 67 | 97 | | 55 | 97 | | 96 |
| KNbO ₃ /KTaO ₃ | Cm | 76 | 49 | 66 | | 70 | 66 | | 103 |
| KNbO ₃ /NaNbO ₃ | <i>Amm2</i> | 61 | 61 | 33i | | 73i, 35i, 20i | 78 | | 50i, 28i |
| PbTiO ₃ /PbZrO ₃ | <i>Cm</i> | 30 | 17 | 21i | | 96i, 15i | 28 | | 77i |
| BaTiO ₃ /BaZrO ₃ | <i>Amm2</i> | 91 | 66 | 87 | | 60i | 89 | | 54i |
| SrZrO ₃ /SrTiO ₃ | <i>P4mm</i> | 58 | 29 | 112i | | 119i, 116i | 47 | | 118i |
| | | Γ | Z | X | Y | S | U | T | R |
| PbTiO ₃ /SrTiO ₃ | <i>Pmm2</i> | 63 | 43 | 30 | 49 | 55i, 33i, 20i | 50 | 51 | 29i |
| PbZrO ₃ /BaZrO ₃ | <i>Pmm2</i> | 51 | 40 | 41 | 28 | 37i, 37i, 28i | 38 | 33 | 7i |
| PbTiO ₃ /BaTiO ₃ | Pmm2 | 53 | 39 | 51 | 53 | 57 | 52 | 54 | 60 |
| BaTiO ₃ /CaTiO ₃ | <i>Pmm2</i> | 122 | 62 | 57 | 106 | 59i, 40i, 21i | 71 | 105 | 55i, 17i |

Amm2 phase for the PbTiO₃/BaTiO₃ superlattice was also characterized by positive frequencies of all optical phonons at the Γ point but manifested a mechanical instability ($C_{12} > C_{11} = C_{22}$).

Table 3 presents the results obtained from calculations of the phonon frequencies at the center of the Brillouin zone and at five high-symmetry points at its boundary for the “ferroelectric ground state” in all the investigated free-standing superlattices. It follows from the table that, for only three of these superlattices, namely, BaTiO₃/SrTiO₃, PbTiO₃/BaTiO₃, and KNbO₃/KTaO₃, the frequencies of all modes at all points of the Brillouin zone are positive (see also Fig. 1b). The verification of the mechanical stability of the determined structures for these three superlattices confirms that they correspond to the true ground states. For the other seven superlattices, a few modes in phonon spectra at the boundary of the Brillouin zone are unstable simultaneously and the search for the true ground state requires consideration of more complex structures.

As follows from Table 3 (see also Fig. 2b), the strongest instability in the “ferroelectric ground state” of the seven remaining superlattices is associated with phonons at the $M(S)$ and $A(R)$ points of the Brillouin zone. The instability of these phonons is usually attributed to the instability of the perovskite structure with respect to the rotation of the oxygen octahedra. Therefore, the search for the ground state for the seven remaining superlattices was continued. The found “ferroelectric ground states” served as a starting point; however, the unit cell volume was doubled and distortions that corresponded to the rotation of the oxygen octahedra and were described by phonons at the M point were added to the structure. The translation vec-

tors in the new unit cell with the double volume and the vectors of the parent lattice are related by the expressions $\mathbf{a}'_1 = \mathbf{a}_1 + \mathbf{a}_2$, $\mathbf{a}'_2 = \mathbf{a}_1 - \mathbf{a}_2$, and $\mathbf{a}'_3 = \mathbf{a}_3$. For this new unit cell, the volume of the Brillouin zone decreases by a factor of two and the M , A , X , and R points of the initial Brillouin zone are mapped into the Γ , Z , M , and A points of the “folded” Brillouin zone, respectively; the Z point in this case remains in place. Since the structural relaxation, as a rule, leads to an increase in the stability of phonons, it is sufficient to trace the change in the frequency of the phonons unstable in the “ferroelectric ground state” during the search for the ground state.

After the relaxation of atomic positions and the unit cell parameters, the polar *Amm2* phase for the free-standing superlattices KNbO₃/NaNbO₃ and BaTiO₃/BaZrO₃ transforms to the phase with space group *Pmc2*₁ (in the setting *P2*₁*am*) in which the polarization vector is oriented along the 2₁ axis (or in the $\langle 110 \rangle$ direction of the parent tetragonal lattice). The *Cm* phase for the PbTiO₃/PbZrO₃ superlattice transforms to the phase with space group *Pc* (in the setting *Pa*) with the polarization vector oriented in the $\langle xxz \rangle$ direction of the parent tetragonal lattice at an angle of 28.4° with respect to the xy plane. It follows from Table 4 that, in the aforementioned phases, the frequencies of all phonons at all points of the Brillouin zone are positive and the structures themselves are mechanically stable. The structure of the other superlattices after the “inclusion” of the structural distortions undergoes more complex transformations.

It turned out that, in the free-standing superlattices PbTiO₃/SrTiO₃ and PbZrO₃/BaZrO₃, the structure with space group *Amm2*, which is formed when rotations of the oxygen octahedra are added to the polar

phase of the “ferroelectric ground state” $Pmm2$, even though has a lower energy, it is not stable: in the phonon spectrum of this structure, the unstable ferroelectric mode is observed at the Γ point with the displacements perpendicular to the current direction of the polarization. The search for the structures with a lower energy leads to the polar $Pmc2_1$ phase, which has the lowest energy for the considered superlattices. It follows from Table 4 and Fig. 2c that, in this phase, the frequencies of all phonons at the Brillouin zone center and high-symmetry points at the Brillouin zone boundary are positive, and the analysis of the elastic moduli indicates that this phase is mechanically stable. Therefore, the $Pmc2_1$ structure is the true ground state of these two superlattices.

For the free-standing superlattices $PbTiO_3/SrTiO_3$ and $PbZrO_3/BaZrO_3$, it is unusual that the most stable phase in the “ferroelectric ground state” is the phase with the polarization vector \mathbf{P}_s parallel to the $\langle 100 \rangle$ axis of the parent tetragonal lattice, whereas the polarization vector \mathbf{P}_s in the true ground state is parallel to the $\langle 110 \rangle$ axis; i.e., the polarization vector rotates in the xy plane through an angle of 45° . This suggests that, with the inclusion of the structural distortions, the polarization direction in the true ground state is not necessarily inherited from the “ferroelectric ground state.” Even more complex change in the polarization direction with the inclusion of the structural distortions is observed in the $SrZrO_3/SrTiO_3$ and $BaTiO_3/CaTiO_3$ superlattices.

The search for the ground state of the free-standing superlattice $SrZrO_3/SrTiO_3$ turned out to be the most complicated problem. The $P4bm$ phase formed from the polar $P4mm$ phase of the “ferroelectric ground state” after the inclusion of the distortions described by phonons at the M point of the Brillouin zone relaxes to the *nonpolar* $P4/mbm$ phase. In the phonon spectrum of this phase, two unstable phonons with symmetry E_u and E_g are observed at the Γ point of the “folded” Brillouin zone (Table 4). The unstable mode with a frequency of $119i \text{ cm}^{-1}$ is a ferroelectric mode and is characterized by the polarization of vibrations in the xy plane. After the addition of the distortions corresponding to the eigenvector of this mode to the structure and the structural relaxation, we obtain the phase with space group Pm , in which the direction of the polarization vector is close to the $\langle 110 \rangle$ direction of the parent lattice (the phase with space group $Pmc2_1$, in which the polarization vector exactly coincides with the $\langle 110 \rangle$ direction, has a somewhat higher energy). The calculations of the phonon spectrum of the Pm phase revealed two unstable phonons with symmetry A'' at the Γ point (Table 4). After the addition of the distortions corresponding to the least stable among these unstable modes to the structure with space group Pm and the structural relaxation, we obtain the phase with space group Pc , for which the frequencies of all phonons at all points of the Brillouin zone are positive

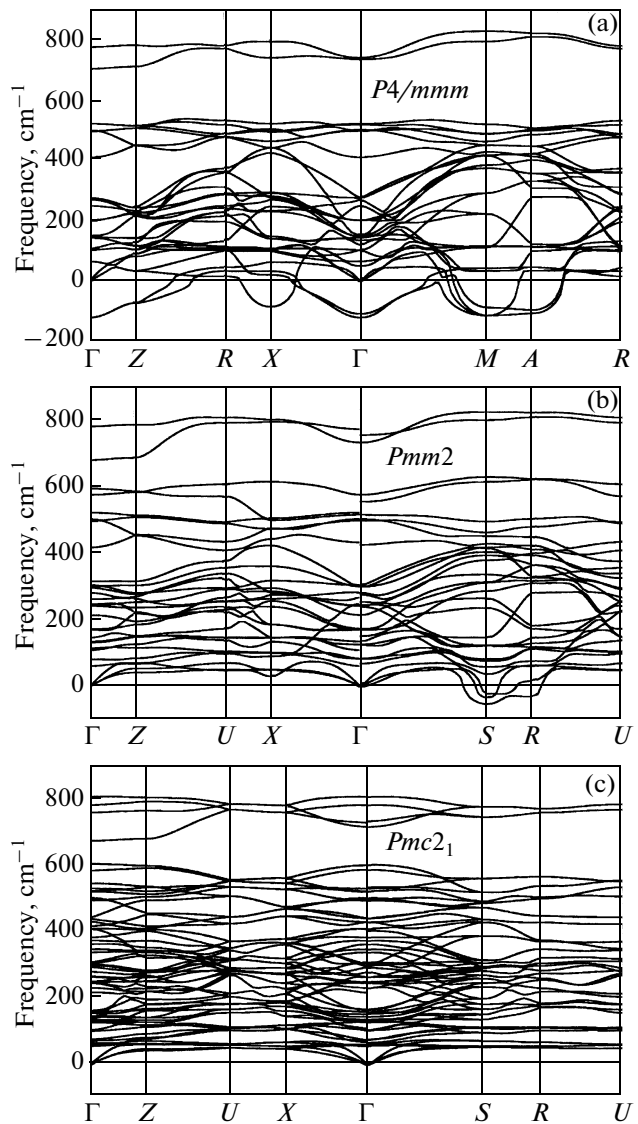


Fig. 2. Phonon spectrum of the free-standing superlattice $(PbTiO_3)_1(SrTiO_3)_1$ in (a) the paraelectric phase $P4/mmm$, (b) the “ferroelectric ground state,” i.e., the $Pmm2$ phase; and (c) the ground state, i.e., the $Pmc2_1$ phase.

(Table 4) and the structure itself is mechanically stable. Therefore, the Pc phase corresponds to the true ground state. The polarization vector in this phase has the $\langle xxz \rangle$ direction and makes an angle of 12.2° with the xy plane; i.e., with the inclusion of the structural distortions, the vector \mathbf{P}_s is strongly tilted with respect to the plane.

The free-standing superlattice $BaTiO_3/CaTiO_3$ is one more system that appeared to be difficult to analyze. In this superlattice, the “ferroelectric ground state” is the $Pmm2$ phase. The phonon spectrum of this phase indicates that the structure is unstable with respect to the distortions described by phonons at the S and R points (Table 3). However, neither the $Amm2$

Table 4. Frequencies of optical phonons at different points of the “folded” Brillouin zone of the superlattices in which the “ferroelectric ground state” is characterized by the presence of unstable optical phonons at the Brillouin zone boundary (the space groups corresponding to the true ground state of the superlattices are printed in boldface)

| Superlattice | Space group | Phonon frequencies, cm^{-1} | | | |
|---------------------------------|----------------------------|--------------------------------------|-----|-----|-----|
| | | Γ | Z | M | A |
| $\text{KNbO}_3/\text{NaNbO}_3$ | $Pmc2_1$ | 65 | 63 | 71 | 92 |
| $\text{PbTiO}_3/\text{SrTiO}_3$ | $Pmc2_1$ | 56 | 42 | 53 | 52 |
| $\text{PbTiO}_3/\text{PbZrO}_3$ | Pc | 43 | 40 | 47 | 48 |
| $\text{SrZrO}_3/\text{SrTiO}_3$ | $P4/mbm$ | 119i, 70i | — | — | — |
| | Pm | 71i, 52i | — | — | — |
| | Pc | 17 | 55 | 50 | 74 |
| $\text{PbZrO}_3/\text{BaZrO}_3$ | $Pmc2_1$ | 41 | 41 | 49 | 47 |
| $\text{BaTiO}_3/\text{BaZrO}_3$ | $Pmc2_1$ | 84 | 66 | 86 | 89 |
| $\text{BaTiO}_3/\text{CaTiO}_3$ | $Pmc2_1$ | 40i | — | — | — |
| | Pc | 59 | 61 | 93 | 91 |

phase (which was obtained after the addition of rotations of the octahedra to the “ferroelectric ground state”) nor the $Pmc2_1$ phase (in which the polarization vector was additionally tilted in the xy plane by an angle of 45° with respect to its direction in the “ferroelectric ground state”) proved to be stable. The phonon spectrum of the $Pmc2_1$ phase with a lower energy as compared to the $Amm2$ phase was characterized by the presence of the unstable ferroelectric mode with a frequency of $40i \text{ cm}^{-1}$ (polarized in the z direction of the parent tetragonal lattice) at the Γ point (Table 4). The addition of the distortions corresponding to the eigenvector of this mode to the structure with space group $Pmc2_1$ leads to the Pc phase, in which

the polarization vector deviates from the xy plane and makes an angle of 20.1° with it. In this phase, the frequencies of all phonons at all points of the Brillouin zone are positive (Table 4), and the structure itself is mechanically stable. Therefore, the Pc phase corresponds to the true ground state of the free-standing superlattice $\text{BaTiO}_3/\text{CaTiO}_3$.

It is interesting that the true ground state in all the ten superlattices studied in this work is a polar state irrespective of whether the constituent components are paraelectrics, ferroelectrics, or antiferroelectrics.

The influence of structural distortions on the physical properties of the superlattices is illustrated in Table 5. It can be seen that the inclusion of structural distortions in most of cases leads to a decrease in the largest eigenvalue of the dielectric constant tensor and makes this tensor more “isotropic.” However, the most radical change is observed for the spontaneous polarization, which not only decreases in magnitude but also changes its direction for four of the studied superlattices.

For all the considered superlattices, Table 2 presents the values of the enthalpy of mixing ΔH , which was estimated as the half-sum of the difference between the total energy of the $P4/mmm$ phase of the superlattice and the sum of the total energies of the cubic phases (space group $Pm3m$) of the constituting components, i.e., the quantities reduced to the five-atom formula unit. It can be seen that, except for three systems in which the B sites are alternately occupied by Ti and Zr atoms, the enthalpy of mixing ΔH for the other seven superlattices is small, which suggests that, at 300 K, these superlattices will be thermodynamically stable. In the titanate–zirconate systems, the enthalpy of mixing ΔH is considerably higher and correlates well with the relative difference between the lattice parameters $\Delta a/\bar{a}$ of the constituent components

Table 5. Eigenvalues of the static dielectric constant tensor and the magnitude and orientation of the polarization vector (with respect to the axes of the parent tetragonal phase) in the “ferroelectric” and true ground states of the investigated ferroelectric superlattices (the magnitude of P_s is given in C/m^2)

| Superlattice | “Ferroelectric ground state” | | | | True ground state | | | |
|---------------------------------|------------------------------|--------------|--------------|-----------------|-------------------|--------------|--------------|-----------------|
| | ϵ_1 | ϵ_2 | ϵ_3 | P_s | ϵ_1 | ϵ_2 | ϵ_3 | P_s |
| $\text{BaTiO}_3/\text{SrTiO}_3$ | 105.3 | 204.3 | 907.3 | 0.241 (xxz) | 105.3 | 204.3 | 907.3 | 0.241 (xxz) |
| $\text{KNbO}_3/\text{KTaO}_3$ | 82.5 | 122.2 | 197.5 | 0.253 (xxz) | 82.5 | 122.2 | 197.5 | 0.253 (xxz) |
| $\text{KNbO}_3/\text{NaNbO}_3$ | 25.0 | 62.6 | 534.4 | 0.489 ($xx0$) | 28.2 | 41.2 | 334.7 | 0.502 ($xx0$) |
| $\text{PbTiO}_3/\text{SrTiO}_3$ | 41.0 | 206.0 | 207.0 | 0.585 ($x00$) | 60.1 | 130.5 | 197.0 | 0.483 ($xx0$) |
| $\text{PbTiO}_3/\text{PbZrO}_3$ | 23.3 | 110.7 | 123.3 | 0.819 (xxz) | 43.7 | 104.1 | 104.3 | 0.661 (xxz) |
| $\text{SrZrO}_3/\text{SrTiO}_3$ | 22.4 | 281.4 | 281.4 | 0.502 ($00z$) | 46.8 | 72.5 | 85.7 | 0.217 (xxz) |
| $\text{PbZrO}_3/\text{BaZrO}_3$ | 28.2 | 78.8 | 89.7 | 0.480 ($x00$) | 38.1 | 49.9 | 60.2 | 0.394 ($xx0$) |
| $\text{BaTiO}_3/\text{BaZrO}_3$ | 34.7 | 44.5 | 79.7 | 0.259 ($xx0$) | 33.7 | 42.4 | 71.0 | 0.259 ($xx0$) |
| $\text{PbTiO}_3/\text{BaTiO}_3$ | 36.2 | 223.5 | 336.1 | 0.563 ($x00$) | 36.2 | 223.5 | 336.1 | 0.563 ($x00$) |
| $\text{BaTiO}_3/\text{CaTiO}_3$ | 24.5 | 92.8 | 95.2 | 0.559 ($x00$) | 45.9 | 74.7 | 117.3 | 0.419 (xxx) |

(calculations were carried out using the lattice parameters a for the cubic phases with space group $Pm\bar{3}m$). This clearly indicates that high enthalpy of mixing in these cases is due to strong internal strains in the superlattices. It is interesting to note that, despite the large ratio $\Delta a/\bar{a}$ for the $\text{BaTiO}_3/\text{CaTiO}_3$ superlattice, the enthalpy of mixing ΔH remains rather small.

As follows from the calculations performed in [25], one of the methods used to decrease the enthalpy of mixing in superlattices of the titanate–zirconate systems can be their growth in the $\langle 111 \rangle$ direction. According to our data, the $Fm\bar{3}m$ phase of the $(\text{PbTiO}_3)_1(\text{PbZrO}_3)_1$ superlattice grown in the $\langle 111 \rangle$ direction has the enthalpy of mixing $\Delta H = -20.8$ meV per formula unit. However, in the phonon spectrum of this phase, apart from the unstable ferroelectric mode Γ_{15} ($132i$ cm^{-1}) at the Γ point, there exist two more unstable phonons Γ'_{15} ($161i$ cm^{-1}) and Γ'_{25} ($51i$ cm^{-1}). Nonetheless, the ground state of this superlattice (the $R3$ phase) remains polar ($|P_s| = 0.620$ C/m²). The investigation of the properties of the other superlattices grown in the $\langle 111 \rangle$ direction requires additional calculations, and they will not be considered in the present paper.

4. DISCUSSION OF THE RESULTS

We compare now the results of our calculations with the available experimental and calculated data for ferroelectric superlattices and the corresponding solid solutions.

At present, the $\text{BaTiO}_3/\text{SrTiO}_3$ superlattice is the most experimentally studied superlattice. It is known from the phase diagram of the BaTiO_3 – SrTiO_3 system [62] that the low-temperature phase in the $\text{Ba}_{0.5}\text{Sr}_{0.5}\text{TiO}_3$ solid solution has symmetry $R3m$. The ground state, i.e., the Cm phase, found for the free-standing superlattice $(\text{BaTiO}_3)_1(\text{SrTiO}_3)_1$ in this work is in agreement both with the results of calculations performed by other authors [3, 12, 13, 63, 64] and with the experimental data obtained for solid solutions: with taking into account the tetragonal perturbation determined by the geometry of the superlattice, the polar $R3m$ phase should transform to the Cm phase. The monoclinic polar distortion of the structure of the $\text{BaTiO}_3/\text{SrTiO}_3$ superlattice, which agrees with the results of our calculations, was observed in [9]. A small splitting of the frequencies $E_u - A_{2u}$ in the phonon spectrum of the $P4/mmm$ phase of the superlattice under consideration (Table 2) indicates a sufficiently weak perturbation caused by the mechanical strain of the layers, as well as by the nonequivalence of the environment of the titanium atoms. Nonetheless, the polarization vector appears to be deviated from the $\langle 111 \rangle$ direction of the cube toward the xy plane through an angle of 20.6° . The weak instability of the phonon with symmetry R_{25} in the phonon spectrum of

SrTiO_3 is compensated by a quite stable same phonon in the phonon spectrum of BaTiO_3 [1, 65]; consequently, the ferroelectric instability at the Γ point in the $P4/mmm$ phase is the only instability of the superlattice [3].

According to the results of our calculations, the ground state of the free-standing superlattice $\text{KNbO}_3/\text{KTaO}_3$ is the Cm phase. This result is in agreement with the experimental data for the $\text{KNb}_{0.5}\text{Ta}_{0.5}\text{O}_3$ solid solution, in which the symmetry of the low-temperature phase is $R3m$ [62]. As for the $\text{BaTiO}_3/\text{SrTiO}_3$ superlattice, the found symmetry of the ground state (Cm) with taking into account the tetragonal perturbation determined by the geometry of the superlattice corresponds to the experimentally observed symmetry in the solid solution, even though the splitting of the modes $A_{2u} - E_u$ for this superlattice is larger. The orientation of the polarization vector in this superlattice is considerably closer to the $\langle 111 \rangle$ direction of the cube as compared to the $\text{BaTiO}_3/\text{SrTiO}_3$ superlattice: the deviation of the polarization vector toward the xy plane is equal to 7.2° . The stability of the structures of both constituent components of the superlattice, i.e., KNbO_3 and KTaO_3 , with respect to the rotation of the oxygen octahedra, makes the superlattice structure stable to these distortions.

In order to compare with the results of earlier calculations of the properties of the $\text{KNbO}_3/\text{KTaO}_3$ superlattices [53], we additionally calculated and analyzed the properties of these superlattices supported on the KTaO_3 substrate and superlattices with a larger period. It turned out that our results differ strongly from the results of previous calculations: according to our data, the $P4mm$ phase of the $(\text{KNbO}_3)_1(\text{KTaO}_3)_1$ superlattice supported on the KTaO_3 substrate is unstable (its phonon spectrum contains the ferroelectric mode with symmetry E and frequency of $90i$ cm^{-1}) and the ground state of this superlattice is the Cm phase. Moreover, our calculations for the $(\text{KNbO}_3)_1(\text{KTaO}_3)_3$ superlattice predict the existence of the polar state in both free-standing superlattice (the $Amm2$ phase, the polarization vector is parallel to $\langle 110 \rangle$) and the superlattice supported on the KTaO_3 substrate (the Cm phase, the polarization vector is directed along $\langle xxz \rangle$). In [53], the polar state in the $(\text{KNbO}_3)_1(\text{KTaO}_3)_3$ superlattice supported on the KTaO_3 substrate was not found (for space group $P4mm$).

As regards the antiferroelectric phase discussed in [53] for the $(\text{KNbO}_3)_1(\text{KTaO}_3)_1$ superlattice, it is not clear from the results obtained in [53], in which phase (high-symmetry or ferroelectric) the unstable phonon was found at the X point. According to our calculations for the free-standing superlattice, the phonon spectrum of the Cm phase does not contain this instability (Table 3) and the phonon spectrum of the $P4/mmm$ phase, apart from the ferroelectric instabil-

ity, also contains two unstable phonons at the X point ($71i$, $34i$ cm^{-1}), one unstable phonon at the R point ($61i$ cm^{-1}), and one unstable phonon at the Z point ($126i$ cm^{-1}). However, the instabilities associated with these phonons at the boundary of the Brillouin zone are weaker than the ferroelectric instability ($143i$, $106i$ cm^{-1}). Our results indicate that the formation of the intermediate antiferroelectric phase in the $(\text{KNbO}_3)_1(\text{KTaO}_3)_1$ superlattice is unlikely, as compared to the conclusion made in [51] from the increase in the dielectric constant in the electric field in the temperature range $140\text{--}230^\circ\text{C}$.

Our results for the $\text{PbTiO}_3/\text{BaTiO}_3$ superlattice appeared to be unexpected. It is known that the symmetry of the low-temperature phase in the $\text{Pb}_{0.5}\text{Ba}_{0.5}\text{TiO}_3$ solid solution is $P4mm$ [62]. Our calculations predict that the true ground state of this superlattice has a $Pmm2$ structure with the in-plane orientation of \mathbf{P}_s along the x axis (Table 2); the energies of the $Amm2$ and $P4mm$ phases with the orientation of \mathbf{P}_s along the $\langle 110 \rangle$ and $\langle 001 \rangle$ directions are higher than the energy of the $Pmm2$ phase by 3.7 and 26.2 meV, respectively. We can suppose that the $Pmm2$ phase is the tetragonal polar phase that is observed in solid solutions but in which, for some reason, the polar axis appears to be rotated to the layer plane. Then, taking into account the tetragonal perturbation determined by the geometry of the superlattice, the symmetry of the structure should be lowered exactly to $Pmm2$. This is evidenced by the relationship between the calculated lattice parameters of the $Pmm2$ phase: $a = 7.6366$ Bohr $\gg b = 7.4353$ Bohr $\approx c/2 = 7.4221$ Bohr. In experiments, this orientation of the polarization vector in the $\text{PbTiO}_3/\text{BaTiO}_3$ superlattice is confirmed by the results of Raman scattering investigations [39, 40]; one can add that, in this case, the superlattice remains polar up to 600°C [41].

The structural stability of the $(\text{PbTiO}_3)_1(\text{BaTiO}_3)_1$ superlattice with respect to the rotation of the oxygen octahedra is most likely associated with the high stability of the R_{25} and M_3 modes in BaTiO_3 , which completely compensates for the instability of these modes in the phonon spectrum of PbTiO_3 .

The change in the polarization as a function of the ratio between the thicknesses of PbTiO_3 and BaTiO_3 layers in the $\text{PbTiO}_3/\text{BaTiO}_3$ superlattices supported on the SrTiO_3 substrate was studied from first principles in [42]. In this case, it was assumed that the polar phase has symmetry $P4mm$. According to our calculations, the $P4mm$ phase in the $(\text{PbTiO}_3)_1(\text{BaTiO}_3)_1$ superlattice supported on the SrTiO_3 substrate is unstable: its phonon spectrum contains the unstable ferroelectric mode of symmetry E with a frequency of $23i$ cm^{-1} . The Pm phase is the ground state of this superlattice. In the $(\text{PbTiO}_3)_2(\text{BaTiO}_3)_2$ superlattice, the mode E is even less stable (its phonon frequency is $50i$ cm^{-1}) and the Cm phase, whose energy is only 0.26

meV lower than the energy of the Pm phase, becomes the ground state.

In [39, 40], it was found that, in the $\text{PbTiO}_3/\text{BaTiO}_3$ superlattice, the local lattice parameters in the PbTiO_3 and BaTiO_3 layers differ substantially (by 0.11 Å) in the direction of the z axis perpendicular to the layer plane, which, in the authors' opinion, indicates an unusual matching of layers ($a\text{-PbTiO}_3/c\text{-BaTiO}_3$). However, strong variations in the magnitude and direction of the polarization vector in this matching should necessarily lead to a strong increase in the electrostatic energy, which makes this matching energetically unfavorable. In order to calculate the difference between the lattice parameters in uniformly polarized superlattices, for free-standing $(\text{PbTiO}_3)_2(\text{BaTiO}_3)_2$ and $(\text{PbTiO}_3)_3(\text{BaTiO}_3)_3$ we calculated the structure of the $P4/mmm$, $Pmm2$, $Amm2$, and $P4mm$ phases and determined the lattice parameters in individual layers along the z axis. It turned out that the difference between these lattice parameters, which was estimated from the difference between the Pb–Pb and Ba–Ba distances in the layers, is equal, on average, to 0.10 Å and changes from one polar phase to another polar phase by no more than 0.015 Å. From this it follows that the experimentally observed difference between the lattice parameters is associated not with the unusual matching of layers but is a simple consequence of different sizes of barium and lead atoms.

The result for the “ferroelectric ground state” in the $\text{PbTiO}_3/\text{SrTiO}_3$ superlattice appeared to be very similar to the result for the $\text{PbTiO}_3/\text{BaTiO}_3$ superlattice. The symmetry of the low-temperature phase in the $\text{Pb}_{0.5}\text{Sr}_{0.5}\text{TiO}_3$ solid solution is $P4mm$ [62]. Our calculations predict that the “ferroelectric ground state” of this superlattice has a structure $Pmm2$ (Table 2); the energies of the $Amm2$ and $P4mm$ phases are higher than the energy of the $Pmm2$ phase by 5.8 and 21.3 meV, respectively. As for the $\text{PbTiO}_3/\text{BaTiO}_3$ superlattice, the results of the calculations for the $\text{PbTiO}_3/\text{SrTiO}_3$ superlattice are in agreement with the experimental data for the solid solutions supposing that, for some reason, the polar axis of the tetragonal structure appears to be rotated to the layer plane and taking into account the tetragonal perturbation determined by the geometry of the superlattice. The relationship between the lattice parameters in the $Pmm2$ phase ($a = 7.5324$ Bohr $\gg b = 7.3473$ Bohr $\approx c/2 = 7.3608$ Bohr) agrees with this supposition.

The instability of the R_{25} and M_3 phonons in phonon spectra of both PbTiO_3 and SrTiO_3 [1] is responsible for the instability of the phonon spectrum of the $\text{PbTiO}_3/\text{SrTiO}_3$ superlattice of the $Pmm2$ phase at the S point of the Brillouin zone (Fig. 2b), and the $Pmc2_1$ phase appears to be the true ground state of this superlattice (Table 4, Fig. 2c). This conclusion regarding the symmetry of the ground state of the free-stand-

ing superlattice $(\text{PbTiO}_3)_1(\text{SrTiO}_3)_1$ is in agreement with the results of the calculations performed in [21].

With the aim of comparing with the results of the calculations carried out in [18, 19, 21] for the $\text{PbTiO}_3/\text{SrTiO}_3$ superlattices supported on the SrTiO_3 substrates, in the present work, we performed a series of calculations for similar structures. In the analysis of the properties of these superlattices, the authors of [18, 19] restricted themselves to consideration only of the $P4mm$ phase, and among the polar phases neglecting the rotation of the oxygen octahedra, only the $P4mm$ and $Amm2$ phases were examined in [21]. In none of these papers, the stability of the found structures was checked. Our calculations showed that, in the phonon spectrum of the $(\text{PbTiO}_3)_1(\text{SrTiO}_3)_1$ superlattice supported on the SrTiO_3 substrate, the unstable ferroelectric mode of symmetry E with a frequency of $60i \text{ cm}^{-1}$ occurs at the Γ point. Among the phases neglecting the rotation of the oxygen octahedra, the Cm phase with the polarization vector oriented in the $\langle xxz \rangle$ direction has the lowest energy and the Pm phase with the $\langle x0z \rangle$ orientation of the polarization vector has an energy that is higher by only 0.03 meV . For the four-layered superlattices $(\text{PbTiO}_3)_1(\text{SrTiO}_3)_3$, $(\text{PbTiO}_3)_2(\text{SrTiO}_3)_2$, and $(\text{PbTiO}_3)_3(\text{SrTiO}_3)_1$ supported on the SrTiO_3 substrate, the $P4mm$ phase also turned out to be unstable (the frequencies of the modes of symmetry E are equal to $76i$, $70i$, and $19i \text{ cm}^{-1}$, respectively). The “ferroelectric ground state” for the $(\text{PbTiO}_3)_1(\text{SrTiO}_3)_3$ superlattice is the Pm phase (\mathbf{P}_s is directed along $\langle x0z \rangle$), and the “ferroelectric ground state” for the other two superlattices is Cm (\mathbf{P}_s is directed along $\langle xxz \rangle$). For the subsequent discussion, it is important that, as the number of PbTiO_3 layers in the four-layered superlattices $\text{PbTiO}_3/\text{SrTiO}_3$ increases, the angle between the direction of the polarization vector and the xy plane in the Pm phase monotonically increases from 32.9° for the $(\text{PbTiO}_3)_1(\text{SrTiO}_3)_3$ superlattice to 78.0° for the $(\text{PbTiO}_3)_3(\text{SrTiO}_3)_1$ superlattice and this angle in the Cm phase increases from 34.0° to 73.6° .

The obtained results enable us to explain the cause of the nonmonotonic dependence of the ratio c/a (the measure of the polarization in the direction perpendicular to the substrate), which was experimentally observed with increasing thickness of PbTiO_3 layers in the $\text{PbTiO}_3/\text{SrTiO}_3$ superlattices grown on the SrTiO_3 substrate [18]. In our opinion, this dependence is associated with the manifestation of the structural relaxation and the nonmonotonic dependence of the strains on the ratio between the numbers of PbTiO_3 and SrTiO_3 layers in this superlattice. In thin structures (the $(\text{PbTiO}_3)_1(\text{SrTiO}_3)_3$ superlattice), the substrate produces low strains in the superlattice (Table 6), the critical thickness exceeds the superlattice thickness, and superlattice layers are in the state coherently matched to the substrate. As was shown above, this state is characterized by a noticeable z component of

Table 6. Tangential strains in the film and the z component of the spontaneous polarization in the $(\text{PbTiO}_3)_m(\text{SrTiO}_3)_n$ superlattices and the PbTiO_3 film supported on the SrTiO_3 substrate

| m/n | $(\sigma_{11} + \sigma_{22})/2$, GPa | P_z , C/m ² |
|------------------|---------------------------------------|--------------------------|
| 1/3 | −1.17 | 0.183 |
| 2/2 | −1.77 | 0.301 |
| 3/1 | −0.37 | 0.619 |
| PbTiO_3 | +0.21 | 0.878 |

polarization. As the number of PbTiO_3 monolayers in the superlattice increases, the strains increase, the critical thickness decreases, and, since the total thickness of the structure increases too, the region of the structure the most distant from the substrate begins to relax. In this case, the z polarization component averaged over the volume decreases because, as was demonstrated above, the polarization vector in the relaxed superlattice lies in the film plane. With a further increase in the number of PbTiO_3 monolayers, the strains in the superlattice weaken (Table 6), the structure again becomes coherently matched to the substrate, the tendency toward an increase in the angle of rotation of the polarization vector with respect to the layer plane starts to dominate, and the z component of polarization again increases.

The $\text{PbTiO}_3/\text{PbZrO}_3$ superlattices were among the first experimentally investigated superlattices [23]. The interest to these superlattices is determined, to a large extent, by the search for the reasons of unique ferroelectric and piezoelectric properties of $\text{PbZr}_{1-x}\text{Ti}_x\text{O}_3$ solid solutions [24]. In these solid solutions, the morphotropic boundary between the tetragonal ($P4mm$) and rhombohedral ($R3m$) phases with a thin “layer” of the intermediate monoclinic phase is located at $x = 0.5$ [66]. Our calculations showed that the “ferroelectric ground state” of the $(\text{PbTiO}_3)_1(\text{PbZrO}_3)_1$ superlattice is the Cm phase, in which the polarization vector deviates from the $\langle 111 \rangle$ direction of the cube toward the xy plane by an angle of 11.9° . The instability of the PbTiO_3 and PbZrO_3 structures with respect to rotations of the oxygen octahedra [1, 65] results in the fact that, in the Cm phase, there arise unstable phonons at the M , A , and X points at the boundary of the Brillouin zone (Table 3). The Pc phase (Table 4) with the polarization in the $\langle xxz \rangle$ direction of the parent tetragonal lattice appears to be the true ground state of the superlattice. The results obtained agree with the results of the calculations performed in [27], according to which the Cm phase is the “ferroelectric ground state” of this superlattice; unfortunately, the authors of [27] did not check the stability of the found structure with respect to the phonons at the boundary of the Brillouin zone, even though they admitted the possibility of manifesting this instability.

In the five superlattices considered above, we observed the same phenomenon: in the ground state, the polarization vector \mathbf{P}_s either deviates from the $\langle 111 \rangle$ direction of the cube toward the layer plane or was completely located in this plane. Now, we discuss the reason of this phenomenon. In our opinion, the tendency to the tilt of the polarization vector toward the layer plane is associated with the fact that this leads to the disappearance of the necessity to “maintain” close values of \mathbf{P}_s in the neighboring layers of the superlattice, which are required for decreasing the electrostatic energy of the bound charge $\rho_b = -\nabla \cdot \mathbf{P}_s$. This can be easily verified by comparing the values of P_s in the neighboring layers of the superlattice for two polarization orientations. The estimates obtained for P_s from the displacements of atoms and their effective charges according to the technique described in [10] show that, in the $P4mm$ phase, the values of P_s in the neighboring layers coincide within accuracy of 1% for the $(\text{PbTiO}_3)_1(\text{SrTiO}_3)_1$ superlattice and 7.5% for the $(\text{PbTiO}_3)_1(\text{BaTiO}_3)_1$ superlattice, whereas, in the $Pmm2$ phase, they differ by a factor of 1.56 and 1.75, respectively.

A decrease in the energy of superlattices with the tilt of the polarization vector toward the layer plane can be understood using a simple electrostatic model. When the polarization vector is oriented perpendicular to the layer plane of a superlattice, at the boundaries of two ferroelectrics with different spontaneous polarizations, there appears a surface charge which induces an electric field in both layers so that the electric displacement fields in them are equal to each other. The field-induced change in the polarization in the layers occurs as a result of the displacements of ions from their “equilibrium” positions for these materials. This means that, for such a polarization direction, the total energy of the crystal will be increased by the sum of the energies of the electric field in the layers and the energy of local mechanical strains. The rotation of the polarization vector to the layer plane leads to the disappearance of the aforementioned electric fields and eliminates the necessity of additional ionic displacements, which results in a decrease in the total energy of the system.

An important sequence of the “strained” state in superlattices polarized perpendicular to the layer plane is a *decreased polarization* in the polar phase: in particular, the values of P_s in the $P4mm$ and $Pmm2$ phases for the free-standing superlattices $(\text{PbTiO}_3)_1(\text{SrTiO}_3)_1$ are equal to 0.420 and 0.585 C/m², respectively, and the values of P_s in these phases for the $(\text{PbTiO}_3)_1(\text{BaTiO}_3)_1$ superlattices differ even more strongly: 0.332 and 0.563 C/m². The same strong difference between the values of P_s in the $P4mm$ and $Pmm2$ phases is also observed for the $(\text{BaTiO}_3)_1(\text{CaTiO}_3)_1$ superlattices: 0.335 and 0.559 C/m², respectively.

It should be noted that the above values of P_s for the layers of the $(\text{PbTiO}_3)_1(\text{SrTiO}_3)_1$ superlattice in the $Pmm2$ phase enable us to draw the conclusion regarding relatively strong correlations of the transverse polarization component in the neighboring layers: their values noticeably exceed the correlations determined for the $\text{KNbO}_3/\text{KTaO}_3$ and $\text{BaTiO}_3/\text{SrTiO}_3$ superlattices by the atomic simulation [48, 49]. The probable factor responsible for this difference can be a significant role played by the displacement of lead atoms in the soft mode in PbTiO_3 .

The $\text{SrZrO}_3/\text{SrTiO}_3$ superlattices are of interest because ferroelectricity was first revealed in these superlattices formed from nonpolar constituent components [15, 32, 34]. At low temperatures, the strontium titanate has a structure with space group $I4/mcm$ and the strontium zirconate has a structure with space group $Pbnm$. The $\text{SrTi}_{0.5}\text{Zr}_{0.5}\text{O}_3$ solid solution at 300 K has a structure $I4/mcm$ [67]. According to the results of our calculations, the “ferroelectric ground state” of this superlattice is the $P4mm$ phase. Since both constituent components SrTiO_3 and SrZrO_3 are characterized by the instability with respect to the rotation of the oxygen octahedra, the superlattice itself also exhibits the same instability, and the $P4mm$ phase with the inclusion of these distortions transforms to the Pc phase, which is the true ground state (Table 4). The results of these calculations differ from those obtained in [33, 34], in which the properties of the free-standing superlattices $\text{SrZrO}_3/\text{SrTiO}_3$ were calculated from first principles but only the structure with space group $P4mm$ was considered. It follows from our calculations that, in the phonon spectrum of the $P4mm$ phase of the free-standing superlattice $(\text{SrZrO}_3)_1(\text{SrTiO}_3)_1$, all phonons at the Γ point are stable but several modes at the boundary of the Brillouin zone turn out to be unstable (Table 3). The value of P_s in the $P4mm$ phase is actually large (0.502 and 0.427 C/m² according to our data and data obtained in [34], respectively); however, the inclusion of structural distortions results in a decrease in this value by a factor of 2.3 (Table 5).

We consider now the $\text{BaTiO}_3/\text{BaZrO}_3$ superlattice. It is believed that the barium zirconate retains the cubic structure $Pm3m$ down to 2 K, even though the calculations reveal a weak instability at the R point of the Brillouin zone in its phonon spectrum [68]. The phase diagram of the BaTiO_3 – BaZrO_3 system has been studied to the composition $x = 0.3$ [62]; with an increase in x , the phase transition becomes strongly diffuse and the extrapolation of the phase diagram suggests that the $\text{BaTi}_{0.5}\text{Zr}_{0.5}\text{O}_3$ solid solution at $T \rightarrow 0$ has a cubic or polar rhombohedral structure. At 300 K, the $\text{BaTi}_{0.5}\text{Zr}_{0.5}\text{O}_3$ samples have a cubic structure [69]. The results of our calculations, which predict the ferroelectric phase with space group $Pmc2_1$ as the true ground state of the free-standing superlattice $\text{BaTiO}_3/\text{BaZrO}_3$, differ strongly from the results for

solid solution. An unexpected property revealed for this superlattice in the calculations was the instability of the “ferroelectric ground state” (the *Amm2* phase) with respect to the rotation of the oxygen octahedra, because this instability is absent in BaTiO₃ and weak in BaZrO₃. The existence of the found ground state with the in-plane polarization is confirmed by the experiments in which the hysteresis loops in superlattices were observed for a planar arrangement of electrodes on the film surface [15] but were almost absent in short-period superlattices for a “vertical” arrangement of electrodes [38].

In [38], the authors consider the problem of the mechanical strain relaxation in the BaTiO₃/BaZrO₃ pair superlattices with thick layers. According to their estimates, the critical thickness for the BaTiO₃/MgO ($\Delta a/\bar{a} \approx 5.2\%$) is approximately equal to 15 Å. Since all titanate–zirconate systems are characterized by close mismatches of the lattice parameters (Table 2), one can expect that the critical thickness in these superlattices should be close to the above value. The BaTiO₃/BaZrO₃ superlattices in which the periods varied from 32 to 80 Å were investigated in [38]. It seems likely that the thinnest films remain coherently strained and the polarization in them lies in the *xy* plane. With an increase in the layer thickness, the strains begin to relax and the lattice parameters of the layers tend to values characteristic of bulk samples. With strain relaxation, the polarization in the BaZrO₃ layers disappear and the polarization vector in the BaTiO₃ layers deviates from the film plane. This explains the increase in the *z* component of polarization with an increase in the period of the BaTiO₃/BaZrO₃ superlattice, which was experimentally observed in [38].

Now, we consider the PbZrO₃/BaZrO₃ superlattice. According to the data obtained in [62], the Pb_{0.5}Ba_{0.5}ZrO₃ solid solution has a cubic structure. Our calculations predict that the *Pmm2* phase is the “ferroelectric ground state” of this superlattice. The structural instability of both constituent components with respect to the rotation of the oxygen octahedra leads to the instability of the *Pmm2* phase, in which the symmetry with the inclusion of rotations of octahedra is lowered to *Pmc2*₁ (the true ground state). The theoretical calculations of the properties of this superlattice have never been carried out previously.

The KNbO₃/NaNbO₃ superlattice was theoretically investigated only in one work [54], according to which the *Cm* phase is the ground state of the unstrained superlattice. The stability of this phase with respect to the distortions described by the phonons at the boundary of the Brillouin zone was not checked. At the same time, it is known that NaNbO₃ is one of the most structurally complex crystals, which undergoes at least five structural and one ferroelectric phase transition in the temperature range 80–920 K [62].

The instability of its phonon spectrum, which is associated with the phonons at the *M* and *R* points of the Brillouin zone, was investigated using inelastic scattering of neutrons [70]. For this reason, it could be expected that the instability of the phonon spectrum at the boundary of the Brillouin zone will be observed in the KNbO₃/NaNbO₃ superlattice. Indeed, as was confirmed by our calculations (Table 3), the instability of the “ferroelectric ground state” (the *Amm2* phase according to our data) occurs at the *M*, *A*, and *X* points of the Brillouin zone. The phase with space group *Pmc2*₁ is the true ground state of the free-standing KNbO₃/NaNbO₃ superlattice. These results differ substantially from the experimental data for the K_{0.5}Na_{0.5}NbO₃ solid solution, which at a low temperature has a rhombohedral structure *R3m* [62] or structure *R3c* in which rotations of octahedra are superimposed on polar displacements [71]. No experimental data on the properties of this superlattice are available in the literature.

According to our data, the *Pmm2* phase is the “ferroelectric ground state” of the free-standing (BaTiO₃)₁(CaTiO₃)₁ superlattice. As a result of strong instability of cubic CaTiO₃, this phase is also unstable and, with the inclusion of the structural distortions, transforms to the *Pc* phase with the polarization vector that makes an angle of 20.1° with the *xy* plane. Unfortunately, the Ba_{0.5}Ca_{0.5}TiO₃ solid solution is not single-phase [62] and the found ground state cannot be compared with data for solid solutions. The results of our calculations differ from the results of theoretical calculations for the BaTiO₃/CaTiO₃ superlattices supported on the SrTiO₃ substrate [43], in which the authors considered only the polar *P4mm* phase without check of its stability. Our calculations for the (BaTiO₃)₁(CaTiO₃)₁ superlattice supported on the SrTiO₃ substrate showed that the unstable ferroelectric mode of symmetry *E* with a frequency of 92i cm⁻¹ is observed in the *P4mm* phase and the “ferroelectric ground state” is the *Pm* phase with the polarization vector that makes an angle of 12.4° with the *xy* plane. The calculated value of the *z* component of polarization (0.083 C/m²) agrees well with the quantity $P_s = 0.085$ C/m² determined from measurements of the parameters of the dielectric hysteresis loops for the electric field applied perpendicular to the layer plane [44].

In [21], the authors discussed the mechanism of appearance of improper ferroelectricity in (PbTiO₃)₁(SrTiO₃)₁ superlattices supported on the SrTiO₃ substrate. This mechanism consisted in appearing the *z* component of polarization due to the simultaneous condensation of two unstable modes of symmetry *M*₂ and *M*₄' at the *M* point of the Brillouin zone of the paraelectric phase *P4/mmm*. This conclusion was based on the fact that the direct product of the irreducible representations of these modes transforms

according to the same irreducible representation as the z component of polarization vector (A_{2u} at the Γ point).

The analysis of our results obtained for the $(\text{PbTiO}_3)_1(\text{SrTiO}_3)_1$ superlattice demonstrates that, despite the presence of the unstable phonons of symmetry M_2 and M'_4 at the M point in the $P4/mmm$ phase of the free-standing superlattice, no polarization along the z axis arises in the ground state. For the same superlattice supported on the SrTiO_3 substrate, the z component of polarization appears before the inclusion of rotations of the oxygen octahedra and, hence, conclusive arguments in support of the proposed mechanism in this case are absent too. The origin why the discussed mechanism of appearance of the z component of polarization may not work is most likely associated with strong competition between different instabilities, owing to which the structural distortion according to one of them results in that phonons corresponding to other instabilities become stable.

In our calculations, there was only one situation, i.e., the $\text{BaTiO}_3/\text{CaTiO}_3$ superlattice, when the inclusion of rotations of octahedra resulted in the appearance of the z component of polarization (Table 5). The analysis shows that the unstable modes of symmetry M'_4 and M_2 at the M point of the $P4/mmm$ phase of the free-standing superlattice with frequencies of $113i$ and $74i$ cm^{-1} remain unstable in the “ferroelectric ground state,” namely, the $Pmm2$ phase (the modes with frequencies of $59i$ and $21i$ cm^{-1} at the S point, Table 3). In essence, the transition to the $Pmc2_1$ phase is accompanied by freezing the distortions described by the mode M_2 of the $P4/mmm$ phase. The eigenvector of the only unstable phonon in the $Pmc2_1$ phase involves antiphase rotations of octahedra in the neighboring layers (corresponding to the mode M'_4 of the $P4/mmm$) phase and polar displacements of Ca and Ba atoms along the z axis. After the structural relaxation, strong antiphase rotations of octahedra in the neighboring layers arise in the structure and the polarization vector deviates from the xy plane. Therefore, the distortions observed in the structure of the $(\text{BaTiO}_3)_1(\text{CaTiO}_3)_1$ superlattice after the inclusion of structural distortions are consistent with the mechanism proposed in [21].

Summing up the results obtained, we can argue that the experimental data available in the literature on the structure of solid solutions cannot serve as a reliable basis for the prediction of the ground state of ferroelectric superlattices. The strain in layers, nonequivalence of the environment of atoms, and tendency of the system toward a decrease in the electrostatic energy of the boundary of two different ferroelectrics are responsible for the discrepancy between the ground states in superlattices and solid solutions and for different orientations of the polarization vector in

these states. The structural distortions that arise as a result of the existence of unstable phonons at the boundary of the Brillouin zone can also lead to a substantial change in the properties of superlattices, including the change in the direction of the polarization vector.

The observed tendency toward the tilt of the polarization vector to the layer plane in superlattices, whose origin was explained above, can complicate the use of superlattices in applications in which the polarization is switched by an electric field applied perpendicular to the film plane. The solution that can help in this case consists in growing thin superlattice films on substrates that induce biaxial compression in films. As follows from the calculations and is confirmed by experiments, the polarization vector under these conditions is predominantly oriented in the direction perpendicular to the substrate.

5. CONCLUSIONS

Thus, in this work, the crystal structure of the ground state of ten ferroelectric superlattices based on crystals with the perovskite structure ($\text{BaTiO}_3/\text{SrTiO}_3$, $\text{PbTiO}_3/\text{SrTiO}_3$, $\text{PbTiO}_3/\text{PbZrO}_3$, $\text{SrZrO}_3/\text{SrTiO}_3$, $\text{PbZrO}_3/\text{BaZrO}_3$, $\text{BaTiO}_3/\text{BaZrO}_3$, $\text{PbTiO}_3/\text{BaTiO}_3$, $\text{BaTiO}_3/\text{CaTiO}_3$, $\text{KNbO}_3/\text{KTaO}_3$, and $\text{KNbO}_3/\text{NaNbO}_3$) was calculated from first principles within the density functional theory. The ground state of all the considered superlattices was found to be ferroelectric. It was revealed that the polarization vector has a tendency toward a tilt to the plane of superlattice layers; this is associated with the decrease in the electrostatic and elastic energy of the system consisting of materials with different ferroelectric properties for this orientation of the polarization vector. The importance of the inclusion of structural distortions associated with unstable phonons at the Brillouin zone boundary, which, in a number of cases, lead to significant changes in ferroelectric and dielectric properties of the superlattices, was demonstrated. The results of the calculations are in good agreement with available experimental data.

Calculations in this work were performed on a laboratory computer cluster (16 cores) and the SKIF-MGU Chebyshev supercomputer.

ACKNOWLEDGMENTS

This work was supported by the Russian Foundation for Basic Research (project no. 08-02-01436).

REFERENCES

1. A. I. Lebedev, *Fiz. Tverd. Tela* (St. Petersburg) **51** (2), 341 (2009) [*Phys. Solid State* **51** (2), 362 (2009)].
2. A. I. Lebedev, *Fiz. Tverd. Tela* (St. Petersburg) **51** (4), 757 (2009) [*Phys. Solid State* **51** (4), 802 (2009)].

3. A. I. Lebedev, *Fiz. Tverd. Tela (St. Petersburg)* **51** (11), 2190 (2009) [*Phys. Solid State* **51** (11), 2324 (2009)].
4. H. Tabata, H. Tanaka, and T. Kawai, *Appl. Phys. Lett.* **65**, 1970 (1994).
5. B. D. Qu, M. Evstigneev, D. J. Johnson, and R. H. Prince, *Appl. Phys. Lett.* **72**, 1394 (1998).
6. T. Zhao, Z.-H. Chen, F. Chen, W.-S. Shi, H.-B. Lu, and G.-Z. Yang, *Phys. Rev. B: Condens. Matter* **60**, 1697 (1999).
7. T. Shimuta, O. Nakagawara, T. Makino, S. Arai, H. Tabata, and T. Kawai, *J. Appl. Phys.* **91**, 2290 (2002).
8. A. Q. Jiang, J. F. Scott, H. Lu, and Z. Chen, *J. Appl. Phys.* **93**, 1180 (2003).
9. S. Rios, A. Ruediger, A. Q. Jiang, J. F. Scott, H. Lu, and Z. Chen, *J. Phys.: Condens. Matter* **15**, L305 (2003).
10. J. B. Neaton and K. M. Rabe, *Appl. Phys. Lett.* **82**, 1586 (2003).
11. L. Kim, D. Jung, J. Kim, Y. S. Kim, and J. Lee, *Appl. Phys. Lett.* **82**, 2118 (2003).
12. K. Johnston, X. Huang, J. B. Neaton, and K. M. Rabe, *Phys. Rev. B: Condens. Matter* **71**, 100103 (2005).
13. J. Lee, L. Kim, J. Kim, D. Jung, and U. V. Waghmare, *J. Appl. Phys.* **100**, 051613 (2006).
14. B. Strukov, S. Davitadze, V. Lemanov, S. Shulman, Y. Uesu, S. Asanuma, D. Schlom, and A. Soukiassian, *Ferroelectrics* **370**, 57 (2008).
15. T. Harigai, S.-M. Nam, H. Kakemoto, S. Wada, K. Saito, and T. Tsurumi, *Thin Solid Films* **509**, 13 (2006).
16. J. H. Lee, J. Yu, and U. V. Waghmare, *J. Appl. Phys.* **105**, 016104 (2009).
17. J. C. Jiang, X. Q. Pan, W. Tian, C. D. Theis, and D. G. Schlom, *Appl. Phys. Lett.* **74**, 2851 (1999).
18. M. Dawber, C. Lichtensteiger, M. Cantoni, M. Veithen, P. Ghosez, K. Johnston, K. M. Rabe, and J.-M. Triscone, *Phys. Rev. Lett.* **95**, 177601 (2005).
19. Z. Zhu, B. Wang, H. Wang, Y. Zheng, and Q. K. Li, *Solid-State Electron.* **50**, 1756 (2006).
20. V. R. Cooper, K. Johnston, and K. M. Rabe, *Phys. Rev. B: Condens. Matter* **76**, 020103 (2007).
21. E. Bousquet, M. Dawber, N. Stucki, C. Lichtensteiger, P. Hermet, S. Gariglio, J.-M. Triscone, and P. Ghosez, *Nature (London)* **452**, 732 (2008).
22. H. Wu, A. Liu, L. Wu, and S. Du, *Appl. Phys. Lett.* **93**, 242909 (2008).
23. I. Kanno, S. Hayashi, R. Takayama, and T. Hirao, *Appl. Phys. Lett.* **68**, 328 (1996).
24. G. Sághi-Szabó, R. E. Cohen, and H. Krakauer, *Phys. Rev. B: Condens. Matter* **59**, 12771 (1999).
25. C. Bungaro and K. M. Rabe, *Phys. Rev. B: Condens. Matter* **65**, 224106 (2002).
26. Z. Wu and H. Krakauer, *Phys. Rev. B: Condens. Matter* **68**, 014112 (2003).
27. C. Bungaro and K. M. Rabe, *Phys. Rev. B: Condens. Matter* **69**, 184101 (2004).
28. T. Choi, J.-S. Kim, B. H. Park, and J. Lee, *Integr. Ferroelectr.* **68**, 13 (2004).
29. T. Choi and J. Lee, *Thin Solid Films* **475**, 283 (2005).
30. T. Choi and J. Lee, *Ferroelectrics* **328**, 41 (2005).
31. H.-M. Christen, L. A. Knauss, and K. S. Harshavardhan, *Mater. Sci. Eng., B* **56**, 200 (1998).
32. T. Tsurumi, T. Harigai, D. Tanaka, S. M.-Nam, H. Kakemoto, S. Wada, and K. Saito, *Appl. Phys. Lett.* **85**, 5016 (2004).
33. K. Yang, C. L. Wang, J. C. Li, M. L. Zhao, and X. Y. Wang, *Solid State Commun.* **139**, 144 (2006).
34. K. Yang, C. Wang, J. Li, C. Zhang, R. Zhang, Y. Zhang, Q. Wu, Y. Lv, and N. Yin, *Phys. Rev. B: Condens. Matter* **75**, 224117 (2007).
35. T.-B. Wu and C.-L. Hung, *Appl. Phys. Lett.* **86**, 112902 (2005).
36. C.-L. Hung, Y.-L. Chueh, T.-B. Wu, and L.-J. Chou, *J. Appl. Phys.* **97**, 034105 (2005).
37. T. Tsurumi, T. Ichikawa, T. Harigai, H. Kakemoto, and S. Wada, *J. Appl. Phys.* **91**, 2284 (2002).
38. P. R. Choudhury and S. B. Krupanidhi, *Appl. Phys. Lett.* **92**, 102903 (2008).
39. F. L. Marrec, R. Farhi, M. E. Marssi, J. L. Dellis, M. G. Karkut, and D. Ariosa, *Phys. Rev. B: Condens. Matter* **61**, R6447 (2000).
40. F. L. Marrec, R. Farhi, D. Ariosa, M. E. Marssi, J.-L. Dellis, and M. G. Karkut, *Ferroelectrics* **241**, 125 (2000).
41. F. L. Marrec, R. Farhi, B. Dkhil, J. Chevreul, and M. G. Karkut, *J. Eur. Ceram. Soc.* **21**, 1615 (2001).
42. V. R. Cooper and K. M. Rabe, *Phys. Rev. B: Condens. Matter* **79**, 180101 (2009).
43. S. M. Nakhmanson, K. M. Rabe, and D. Vanderbilt, *Appl. Phys. Lett.* **87**, 102906 (2005).
44. S. S. A. Seo and H. N. Lee, *Appl. Phys. Lett.* **94**, 232904 (2009).
45. H.-M. Christen, L. A. Boatner, J. D. Budai, M. F. Chisholm, L. A. Géa, P. J. Marrero, and D. P. Norton, *Appl. Phys. Lett.* **68**, 1488 (1996).
46. H.-M. Christen, E. D. Specht, D. P. Norton, M. F. Chisholm, and L. A. Boatner, *Appl. Phys. Lett.* **72**, 2535 (1998).
47. E. D. Specht, H.-M. Christen, D. P. Norton, and L. A. Boatner, *Phys. Rev. Lett.* **80**, 4317 (1998).
48. M. Sepliarsky, S. R. Phillpot, D. Wolf, M. G. Stachiotti, and R. L. Migoni, *Phys. Rev. B: Condens. Matter* **64**, 060101 (2001).
49. M. Sepliarsky, S. R. Phillpot, D. Wolf, M. G. Stachiotti, and R. L. Migoni, *J. Appl. Phys.* **90**, 4509 (2001).
50. M. Sepliarsky, S. R. Phillpot, M. G. Stachiotti, and R. L. Migoni, *J. Appl. Phys.* **91**, 3165 (2002).
51. J. Sigman, D. P. Norton, H. M. Christen, P. H. Fleming, and L. A. Boatner, *Phys. Rev. Lett.* **88**, 097601 (2002).
52. J. Sigman, H. J. Bae, D. P. Norton, J. Budai, and L. A. Boatner, *J. Vac. Sci. Technol. A* **22**, 2010 (2004).
53. S. Hao, G. Zhou, X. Wang, J. Wu, W. Duan, and B.-L. Gu, *Appl. Phys. Lett.* **86**, 232903 (2005).
54. Z. Li, T. Lü, and W. Cao, *J. Appl. Phys.* **104**, 126106 (2008).
55. X. Gonze, J.-M. Beuken, R. Caracas, F. Detraux, M. Fuchs, G.-M. Rignanese, L. Sindic, M. Verstraete, G. Zerah, F. Jollet, M. Torrent, A. Roy, M. Mikami,

- P. Ghosez, J.-Y. Raty, and D. C. Allan, *Comput. Mater. Sci.* **25**, 478 (2002).
56. J. P. Perdew and A. Zunger, *Phys. Rev. B: Condens. Matter* **23**, 5048 (1981).
57. A. M. Rappe, K. M. Rabe, E. Kaxiras, and J. D. Joannopoulos, *Phys. Rev. B: Condens. Matter* **41**, 1227 (1990).
58. URL: <http://opium.sourceforge.net/>.
59. N. J. Ramer and A. M. Rappe, *Phys. Rev. B: Condens. Matter* **59**, 12471 (1999).
60. H. J. Monkhorst and J. D. Pack, *Phys. Rev. B: Solid State* **13**, 5188 (1976).
61. *Physics of Ferroelectrics: A Modern Perspective*, Ed. by K. M. Rabe, C. H. Ahn, and J.-M. Triscone (Springer, Berlin, 2007).
62. *Landolt–Börnstein Numerical Data and Functional Relationships in Science and Technology: New Series* (Springer, Berlin, 2001), Group III, Vol. 36A1.
63. L. Kim, J. Kim, U. V. Waghmare, D. Jung, and L. Lee, *Phys. Rev. B: Condens. Matter* **72**, 214121 (2005).
64. L. Kim, J. Kim, D. Jung, J. Lee, and U. V. Waghmare, *Appl. Phys. Lett.* **87**, 052903 (2005).
65. P. Ghosez, E. Cockayne, U. V. Waghmare, and K. M. Rabe, *Phys. Rev. B: Condens. Matter* **60**, 836 (1999).
66. B. Noheda, D. E. Cox, G. Shirane, J. A. Gonzalo, L. E. Cross, and S.-E. Park, *Appl. Phys. Lett.* **74**, 2059 (1999).
67. T. K.-Y. Wong, B. J. Kennedy, C. J. Howard, B. A. Hunter, and T. Vogt, *J. Solid State Chem.* **156**, 255 (2001).
68. A. R. Akbarzadeh, I. Kornev, C. Malibert, L. Bellaiche, and J. M. Kiat, *Phys. Rev. B: Condens. Matter* **72**, 205104 (2005).
69. M. Veith, S. Mathur, N. Lecerf, V. Huch, T. Decker, H. P. Beck, W. Eiser, and R. Haberkorn, *J. Sol–Gel Sci. Technol.* **17**, 145 (2000).
70. I. Tomeno, Y. Tsunoda, K. Oka, M. Matsuura, and M. Nishi, *Phys. Rev. B: Condens. Matter* **80**, 104101 (2009).
71. D. W. Baker, P. A. Thomas, N. Zhang, and A. M. Glazer, *Appl. Phys. Lett.* **95**, 091903 (2009).

Translated by O. Borovik-Romanova